iJRASET
International Journal For Research in Applied Science and Engineering Technology

INTERNATIONAL JOURNAL FOR RESEARCH

IN APPLIED SCIENCE & ENGINEERING TECHNOLOGY

Volume: 6 **Issue:** III **Month of publication:** March 2018

DOI: http://doi.org/10.22214/ijraset.2018.3415

www.ijraset.com

Call: 08813907089 | E-mail ID: ijraset@gmail.com

International Journal for Research in Applied Science & Engineering Technology (IJRASET)
ISSN: 2321-9653; IC Value: 45.98; SJ Impact Factor: 6.887
Volume 6 Issue III, March 2018- Available at www.ijraset.com

2D Simulation Studies on Use of Boundary Layer Trip for Airfoil E216

Vishwas Patel[1], Kenalkumar Tandel[2], Mayur Jalanapurkar[3]
[1, 2, 3,] *Automobile Engineering Department, GIDC Degree Engineering College, India.*

Abstract: ***In a typical low Reynolds number flow over an airfoil, the problem of laminar separation and LSB (laminar separation bubble) is commonly encountered. The presence of LSB leads to increase the boundary layer thickness above it, which results in increased pressure drag and decreased aerodynamic lift. The mechanical turbulators like trip wires, plain trips, zigzag tape, etc., can be effectively used to improve the performance of airfoils at low Reynolds number. In present work airfoil E216 was selected for the numerical studies. Numerical simulations were done for baseline airfoil as well as airfoil with boundary layer trips at Reynolds number of 10^5 and selected angle of attack range 0° to 14°. Baseline airfoil results were compared with available experimental results. Numerical simulations have shown that use of thin trips improves the aerodynamic performance of E216 airfoil for the selected conditions.***

Keywords : ***2D simulations, Airfoil, LSB, Plain trips, Low Reynolds number.***

I. INTRODUCTION

In a typical flow over an airfoil, flow accelerates over the suction side; and there occurs a suction peak (point of minimum pressure) near the leading edge of the airfoil. After the suction peak, pressure gradually increases as the flow travels downstream, and near the trailing edge pressure becomes equal to the static pressure of the ambient air. A negative pressure gradient acts on the boundary layer over the upper surface of the airfoil due to gradual increase in pressure after suction peak.

If the Reynolds number is low, the boundary layer remains laminar along almost entire chord length of the airfoil. Since laminar boundary layers are not enough energetic to resist any significant negative pressure gradient, usually laminar flow separation occurs [1]. Under definite flow conditions, the separated flow while transitioning from laminar flow to turbulent flow may again attach to the airfoil surface and form a LSB (laminar separation bubble). Such bubbles can be generally observed near to the leading edges of the thin airfoils [2]. LSB forms a recirculation region of low pressure air between separation and reattachment locations [3]. The separated flow may not reattach to the surface if the Reynolds number is very low, and hence LSB will not be formed [4].

The pressure measurements on an airfoil surface can be effectively used to find the locations of separation, transition and reattachment points of a LSB [5]. In surface pressure distribution, a constant pressure region indicates a laminar portion of the LSB. The starting point of the constant pressure region indicates the separation point while the termination of the constant pressure region can be used to locate the transition point. A rapid pressure rise due to fluid entrainment occurs during transition of the separated laminar boundary layer to turbulent boundary layer, and finally the actual pressure distribution matches with inviscid pressure distribution. The reattachment point is the location where actual pressure distribution matches with inviscid pressure distribution.

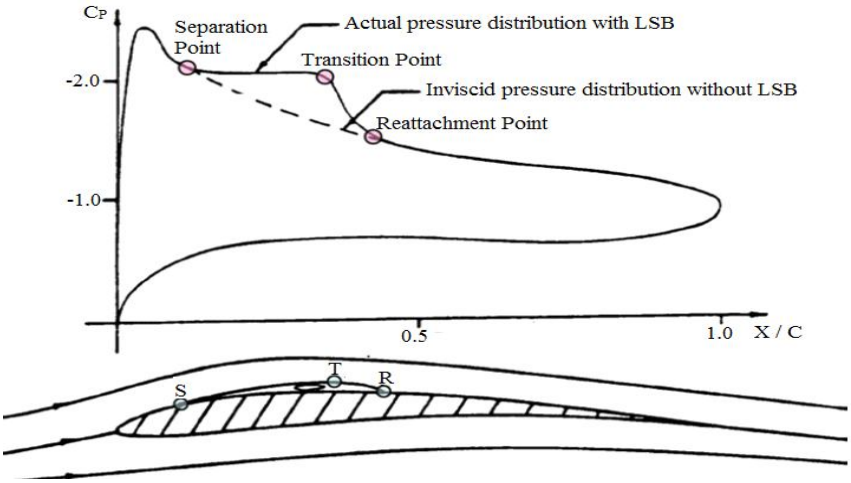

Fig. 1 Laminar separation bubble on an airfoil [5]

The presence of LSB leads to increase the boundary layer thickness above it, which results in increased pressure drag and decreased aerodynamic lift and hence degrades the lift to drag ratio of an airfoil.

A. Use of Boundary Layer Trips

The performance of an airfoil that has a large bubble drag in the baseline configuration can be improved with use of mechanical turbulators like boundary layer trips [6]. Application of trip on airfoil surface has three main effects on drag of airfoil:

1) It reduces bubble drag by eliminating laminar separation bubble as trip converts laminar flow into turbulent flow.
2) It increases the device drag as trip acts as disturbance to the flow.
3) It increases skin friction drag by converting laminar flow into turbulent flow.

Hence trip can only be effective if reduction in bubble drag is greater than increase in device drag and skin friction drag.

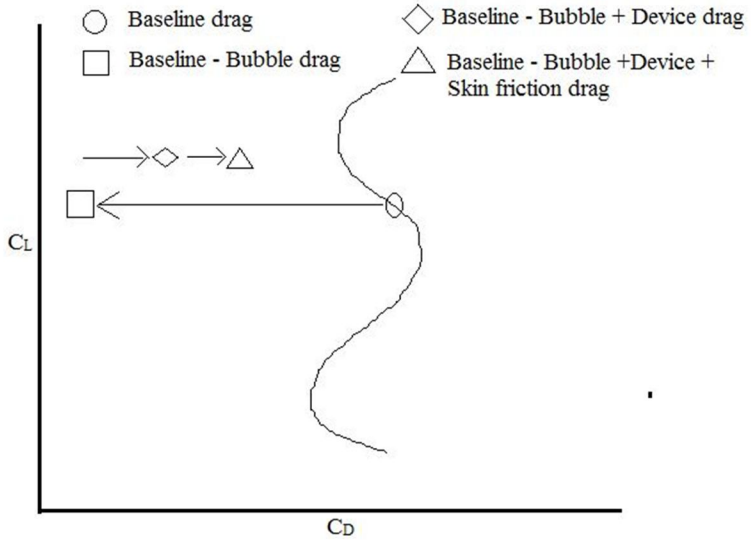

Fig. 2 Conceptual effects of trip on airfoil [6]

For the effective use of the boundary layer trip, it should be placed on the upstream side of the LSB. As the location of the LSB depends on angle of attack of the airfoil while the drag due to LSB depends on the Reynolds number of the flow, and hence trip height and trip location that is effective for one condition might be ineffective for another condition. Though much work is done in this area but it is necessary to test each airfoil separately to know the effect of trip on its aerodynamic performance.

II. METHODOLOGY

In this work 2D numerical simulations are done for flow over an airfoil E216. Simulations are done for baseline airfoil as well as for airfoil with boundary layer trip. Baseline airfoil results obtained using different turbulence models are compared with available results of the experiments. Wind tunnel experiments were performed for baseline airfoil in low speed wind tunnel at Reynolds number of 105 and angles of attack 0° to 14° for recording lift coefficient and drag coefficient data. Oil flow visualisation was also done to determine the location of LSB. The LSB location was found to be approximately at 23% of chord length (i.e. 0.23c) and the same data was used to determine the location of trip to be placed on airfoil while doing the tripped airfoil simulations. All the baseline airfoil simulations are done for Reynolds number of 105 and angle of attack range of 0° to 14° while tripped airfoil simulations are done for same Reynolds number but for only three angles of attack (4°, 6° and 8°). Initially three different turbulent models are used for baseline airfoil simulations and then the model which is in best agreement with baseline experimental results is used for simulations of airfoil with trip. The chord length (c) of airfoil used in simulations is 1m while the trip locations used are 0.2 c (case-1) and 0.12 c (case-2). Different trip heights used at both the trip locations are 6.66mm, 4.66mm, 3.33mm and 2mm. Width of the trip used is 20mm.

A. Two-Dimensional Airfoil Modelling

ICEM is the pre-processor of ANSYS-Fluent. A simulation model can be created in ICEM directly or can be imported from other CAD software packages, such as Solid works and Pro/Engineer. Figure below depicts the profile of E216 airfoil created in ICEM using formatted point data.

ISSN: 2321-9653; IC Value: 45.98; SJ Impact Factor: 6.887
Volume 6 Issue III, March 2018- Available at www.ijraset.com

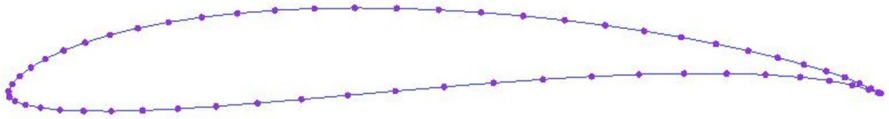

Fig. 3 E216 airfoil profile.

B. Meshing

Two-dimensional meshing was done in pre-processor ICEM. Separate meshes were prepared for different cases (baseline, four different trip heights at two different locations) and unstructured grid was used for all the meshes prepared for simulations. Figures below show computational domain and unstructured mesh around airfoil. A simple rectangle type computational domain was used for all the meshes. The length and width of the computational domain were set to 25 times and 20 times of chord length respectively. In the regions near to the airfoil surface, mesh created was fine enough for the good computational accuracy. As per the requirements of the turbulent models used, the height of the first cell adjacent to the surface was set to 1.8×10^{-4} which resulted in Y^{+} value approximately equal to one.

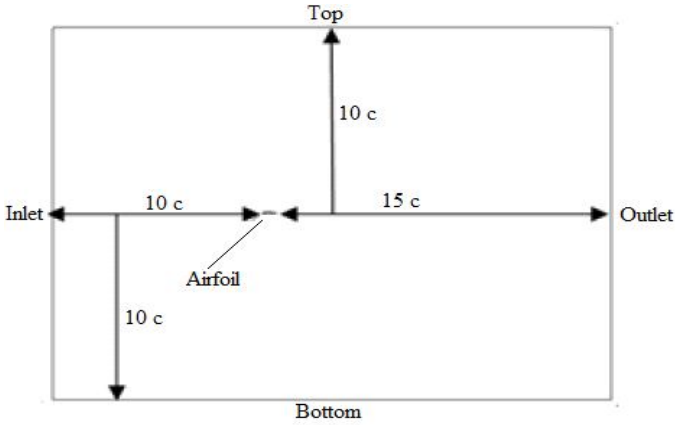

Fig. 4 Computational domain used in simulations

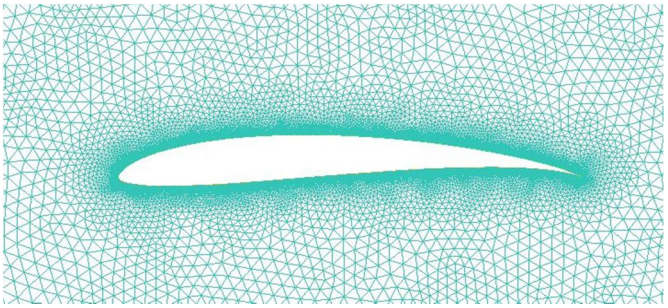

Fig. 5 Figure 5. Airfoil meshing using unstructured grid

Generally as the number of nodes used in meshing is more, the accuracy of the numerical solution increases, but using additional nodes also demands the more computer memory and computational time. Hence grid independency test was done to find optimum number of grid cells in the mesh. Optimum number of grid cells can be found by preparing meshes of different grid cells and running simulations using each mesh. For grid independency test five meshes were prepared with number of grid cells ranging from 200000 to 700000 and simulations were run using SST k-ω model for Reynolds number of 10^5 and angle of attack of 6°. Lift coefficient found from simulations using different meshes is plotted against the number of grid cells. Figure below shows the variation in lift coefficient with number of grid cells in mesh. After approximately 550000 grid cells there was not any significant variation in lift coefficient and hence it was considered as optimum mesh size for all the simulations.

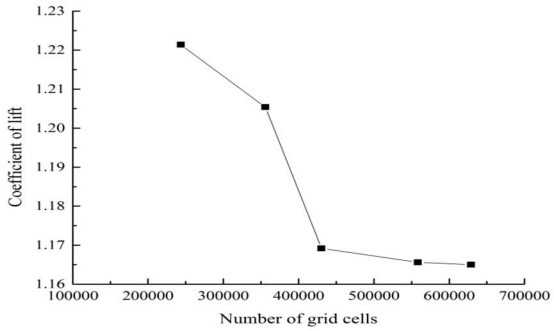

Fig. 6 Effect of number of grid cells on lift coefficient

C. Boundary Conditions and Turbulence Models

Boundary conditions used during all the simulations are as follows: on the airfoil surface no slip and zero pressure conditions are used for the velocity and pressure respectively. On the right side of the domain boundary, pressure outlet boundary conditions are imposed with zero-gauge pressure. For the inlet, top and bottom domain boundaries velocity inlet boundary conditions are considered. Free stream temperature value considered was 308 K, same as the environmental temperature. Kinematic viscosity of air at given temperature is 16.04×10^{-6} m^2/s. At given Reynolds number and free stream air conditions, flow was considered as incompressible. For Reynolds number of 10^5, kinematic viscosity of 16.04×10^{-6} m^2/s and airfoil chord length of 1 m, free stream velocity of air was calculated to be 1.604 m/s. Turbulence models used for baseline airfoil simulations are Spalart-Allmaras model with Vorticity based production, RNG k-ε model with enhanced wall treatment and SST k- ω model with low Reynolds number corrections. For tripped airfoil simulations, only SST k-ω model with low Reynolds number corrections was used.

III. SIMULATION RESULTS

A. Baseline Airfoil Results

Lift coefficient values obtained for different angles of attack from numerical simulations using three different turbulence models are compared with available experimental data. Figure 7 shows the comparison of lift coefficient values between obtained simulation results and experimental results. Though all the three models found to over predict the results for all the angles of attack, lift coefficient values obtained using SST k-ω model are in better agreement with experiments than the ones obtained using RNG k-ε model and Spalart-Allmaras model. Spalart-Allmaras model showed less deviation compared to RNG k-ε model. Stall angle is also correctly predicted by the SST k-ω model while other models failed to do so. For all the models' maximum deviation is found near stall angle and for post-stall angle and this can be attributed to the fact that, around the stall angle, the flow is highly unsteady [7]. Maximum deviation in lift coefficient found from SST k-ω model is 23 % at angle of attack of 14°.

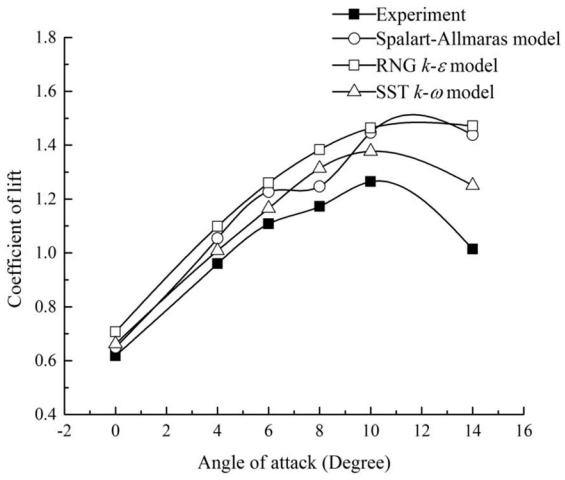

Fig. 7 Comparison of lift coefficient between FLUENT and Experiments

In Figure 8 variation of drag coefficient with angles of attack is shown for all the three turbulence models and experiments. Drag coefficient values are over predicted by RNG k-ε model for all the angles of attack and the model deviated more from experiments compared to other two models. Again SST k-ω model is found in best agreement with experiments. The value is under predicted for angle of attack of 0° and over predicted for remaining angles of attack by the SST k-ω model. Maximum deviation of 10 % with respect to experiments is found for SST k-ω model at angle of attack of 0°. Spalart-Allmaras model also shown good agreement with experiments except at angle of attack of 8°. At stall angle of attack, obtained value of drag coefficient by SST model and Spalart-Allmaras model is very close to experiments.

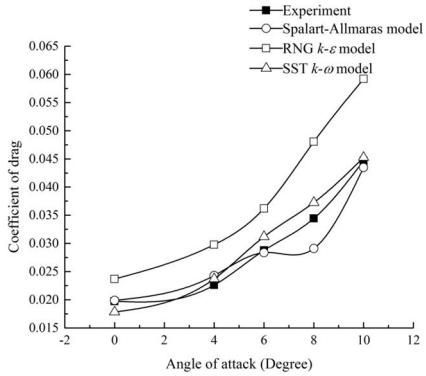

Fig. 8 Comparison of drag coefficient between FLUENT and Experiments

C_L/C_D ratio is calculated using obtained values of C_L and C_D from the simulations. It is clear that deviation of C_L/C_D ratio from experiments is due to cumulative effect of deviation of C_L and deviation of C_D from the experiments. As discussed earlier, deviation of SST k-ω model was least for both C_L and C_D among all the models used which resulted in least deviation in C_L/C_D ratio compared to other models.

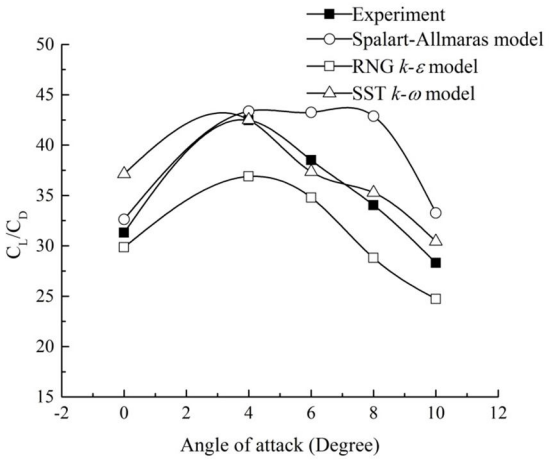

Fig. 9 Comparison of C_L/C_D ratio between FLUENT and Experiments

From above discussions it is clear that SST k-ω model gave least deviations from experiments in the prediction of C_L, C_D and C_L/C_D ratio and hence for the simulations of tripped airfoil only this model is used to see the effect of boundary layer trip on airfoil performance.

B. Tripped airfoil results

In this section effect of boundary layer trip on airfoil performance is discussed on the basis of simulation results. Simulations are performed for two different trip locations 0.2 c (case-1) and 0.12 c (case-2). At both the locations trip heights used are 2 mm, 3.33 mm, 4.66 mm and 6.66 mm. SST k-ω model with low Reynolds number correction is used for the simulations.

Figure 10 shows the simulation results obtained for variation in drag coefficient with trip heights and locations at angle of attack of 4°. Both the cases reduce the drag coefficient compared to baseline for minimum trip height, case-2 also found to slightly reduce

drag coefficient for trip height of 3.33 mm and for the remaining trip location and trip height combinations significant increase in drag coefficient is found. Maximum reduction in drag coefficient obtained is 11 % for case-1 at minimum trip height. Though maximum reduction in drag is found for case-1, case-2 is proved better than case-1 because at higher trip heights increase in drag is less for case-2. C_L/C_D ratio is also found to improve for both the cases at minimum trip height while for other trip location and trip height combinations C_L/C_D ratio is found to decrease compared to baseline except for case-2 at 3.33 mm trip height (Figure 11). Maximum increase in C_L/C_D ratio found is 15 % for case-1 at minimum trip height. Improvement in C_L/C_D ratio is more than in C_D and this is because increase in lift coefficient caused by the trip at particular trip height and trip location combination. Hence it can be concluded that trip height of 2 mm improves overall performance of airfoil E216 at angle of attack of 4°.

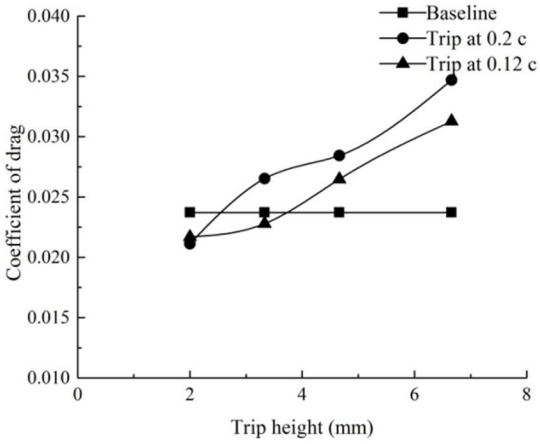

Fig. 10 FLUENT drag data for trips of varying heights at AOA of 4°

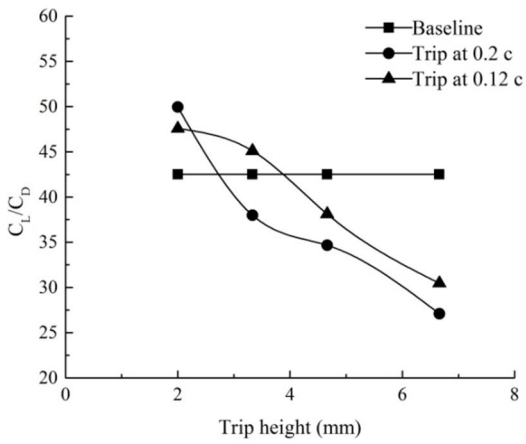

Fig. 11 FLUENT C_L/C_D data for trips of varying heights at AOA of 4°

At angle of attack of 6° both the cases found to reduce drag compared to baseline while using relatively thin trips (Figure 12). For highest trip height both the cases have shown increase in drag compared to baseline. Maximum reduction in drag is found to be 15 % for both the cases at minimum trip height. Figure 13 shows the effect of trip heights and trip location on C_L/C_D ratio at angle of attack of 6°. For C_L/C_D ratio also improvement is found for relatively thin trips. Maximum increase in C_L/C_D ratio found is 21.5 % for case-1 with lowest trip height. Again, reason for more improvement in C_L/C_D ratio compared to C_D is the positive effect of trip on lift coefficient.

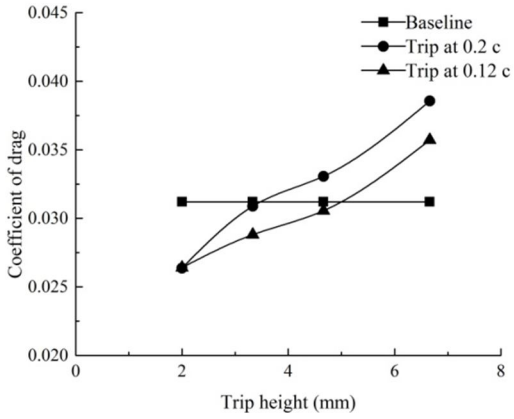

Fig. 12 FLUENT drag data for trips of varying heights at AOA of 6°

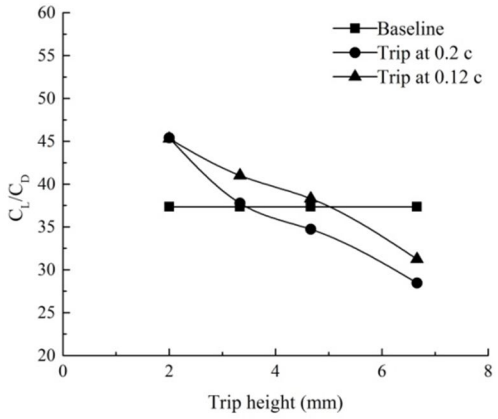

Fig. 13 FLUENT C_L/C_D data for trips of varying heights at AOA of 6°

Figure 14 shows variation in drag coefficient with trip heights and locations at angle of attack of 8°. For case-1 drag coefficient is either reduced or is nearly equal to baseline with all the trip heights except at highest trip height. For case-2 drag coefficient is found

to reduce at minimum trip height while it was nearly equal to baseline for 3.33 mm trip height. Maximum reduction in drag coefficient found is 10 % for case-2 with minimum trip height. C_L/C_D ratio is also found to improve for case-1 with relatively thin trips (Figure 15). Case-2 also improved C_L/C_D ratio at minimum trip height. Maximum increase in C_L/C_D ratio found is 12 % for case-1 at minimum trip height. Least trip height slightly improved the lift coefficient also for both the cases.

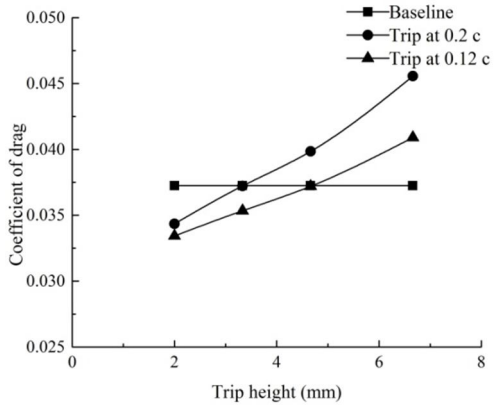

Fig. 14 FLUENT drag data for trips of varying heights at AOA of 8°

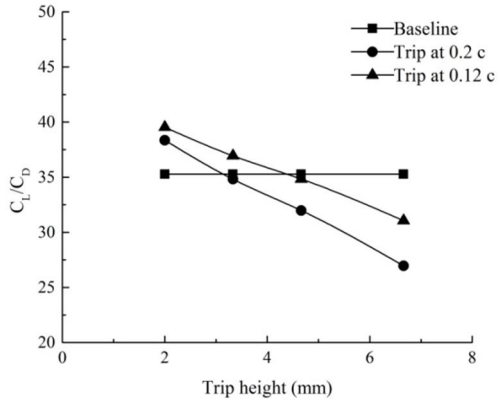

Fig. 15 FLUENT C_L/C_D data for trips of varying heights at AOA of 8°

IV. CONCLUSION

Out of the three different turbulence models used, SST k-ω model was found to be in good agreement with experiments. Tripped airfoil simulations were also done using SST k-ω model and effects of trip on coefficient of drag and C_L/C_D ratio was studied by comparing the results with baseline airfoil simulation results. For trip at location 0.12 c, relatively thin trips were found to improve the performance for all the three angles of attack (4°, 6° and 8°) while for trip at 0.2 c only lowest trip height found to improve performance for all the three angles of attack. Maximum reduction of 15% in drag and maximum increase of 21.5% in ratio was found for angle of attack of 6° while using lowest trip height at location 0.12 c. Trip at 0.12 c was proved to be effective compared to trip at 0.2 c for most of the cases.

REFERENCES

[1] H. Hu and Z. Yang, "An experimental study of the laminar flow separation on a low-Reynolds-number airfoil," Journal of Fluids Engineering, vol. 130, no. 5, pp. 051-101, 2008.
[2] S. S. Diwan and O. N. Ramesh, "On the origin of the inflectional instability of a laminar separation bubble," Journal of Fluid Mechanics, vol. 629, pp. 263-298, 2009.
[3] L. Li, "Experimental Testing of Low Reynolds Number Airfoils for Unmanned Aerial Vehicles," 2013.
[4] A. Gopalarathnam, B. A. Broughton, B. D. McGranahan and M. S. Selig, "Design of low Reynolds number airfoils with trips," Journal of Aircraft, vol. 40, no. 4, pp. 768-775, 2003.
[5] H. Rahimi, W. Medjroubi, B. Stoevesandt and J. Peinke, "2D Numerical Investigation of the Laminar and Turbulent Flow Over Different Airfoils Using OpenFOAM," in Journal of Physics: Conference Series, IOP Publishing, 2014.

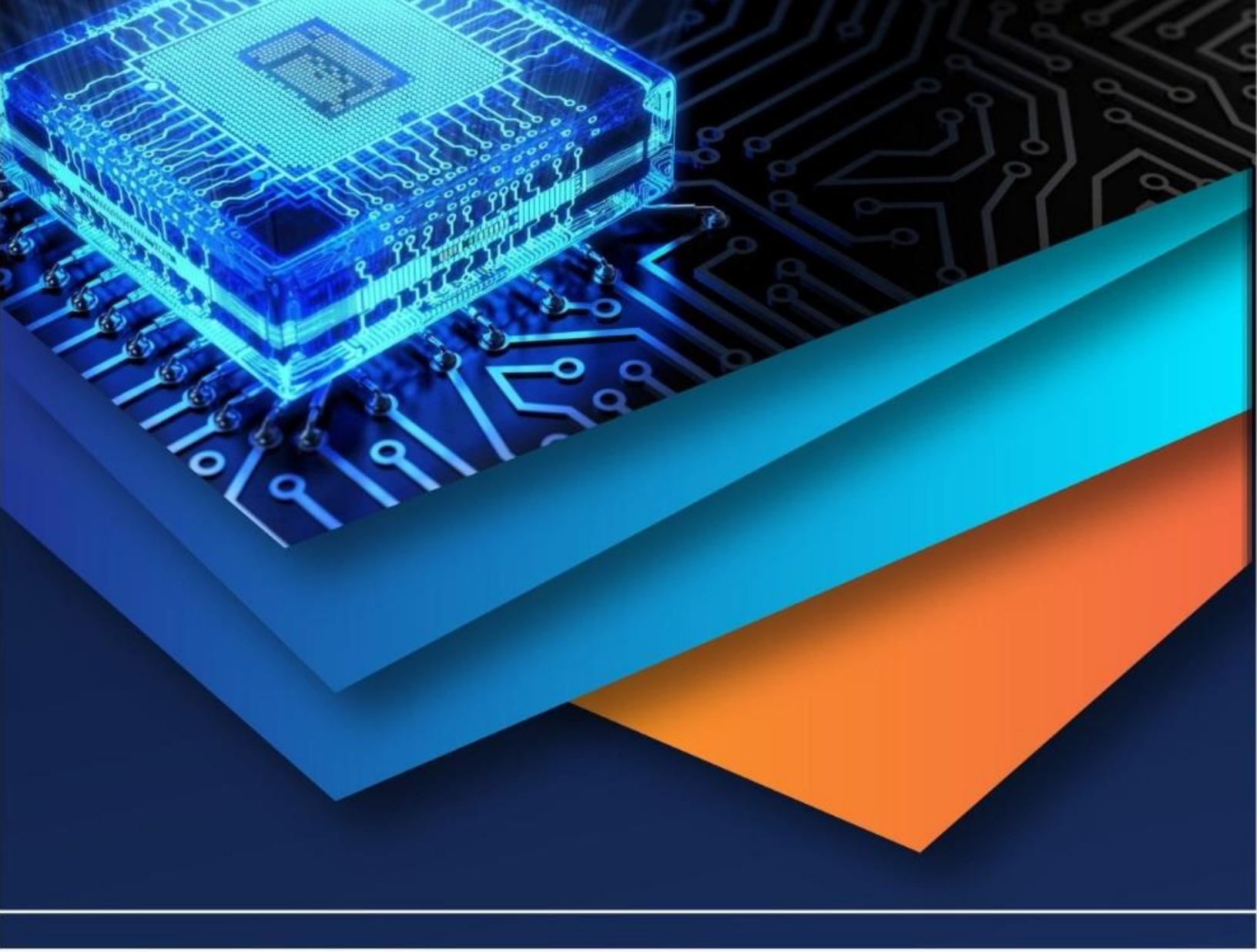

10.22214/IJRASET

45.98

IMPACT FACTOR: 7.129

IMPACT FACTOR: 7.429

INTERNATIONAL JOURNAL FOR RESEARCH

IN APPLIED SCIENCE & ENGINEERING TECHNOLOGY